

The effects of molybdenum trioxide (MoO_3) thickness on the improvement of driving and operating voltages of organic light emitting devices

A. AYOBI^{a,*}, S. N. MIRNIA^a, M. REZAEI ROKNABADI^b, A. BAHARI^a

^aDepartment of Physic, Faculty of Basic Science, University of Mazandaran, Babolsar, Iran

^bDepartment of Physic, Faculty of Science, Ferdowsi University of Mashhad, Mashhad, Iran

In this manuscript, the effects of molybdenum trioxide (MoO_3) thicknesses on the performance of organic light emitting diodes (OLEDs) based on indium tin oxide (ITO) as anode, MoO_3 as hole injection layer (HIL), N-N-diphenyl-N,N-(bis(3-methylphenyl)-1,10-biphenyl-4,40-diamine) (TPD) as hole transport layer (HTL), tris(8-hydroxyquinoline) aluminum (Alq_3) as emission layer (EML) and electron transport layer (ETL), lithium fluoride (LiF) as electron injection layer (EIL), and Aluminum (Al) as cathode have been analyzed. The results show that the MoO_3 leads to the improvement of turn on voltage, current injection and luminance of the OLED devices. Also this material leads to decreasing of the operating and driving voltages, so that the OLED devices with thickness of 5nm for HIL provide the best performance from the point of driving and operating voltages view among all OLEDs fabricated in this work. Thus, this thickness could be considered as the optimal layer thickness.

(Received March 12, 2019; accepted October 9, 2019)

Keywords: Organic, Operating, Voltage, Luminance, Driving, Current, Efficiency

1. Introduction

After the discovery of Organic light emitting diodes (OLEDs) by Tang and VanSlyke in the 1980s [1], these devices have been studied extensively due to influence of the organic fluorescent materials which lead to special properties like high efficiency, light weight, flexibility, potential application in flat panel displays and easy fabrication [2]. Indium tin oxide (ITO) is considered as an appropriate electrode material in such devices because of its high transparency and large conductivity [3]. However, a direct hole-injection from ITO into organic hole transport material can be inefficient in most cases because of a significant energetic mismatch in their interfaces [3,4]. Many researchers have found that energy barrier at the interface between an anode and a hole-transport layer (HTL) is very important in fabricating highly efficient and reliable OLED devices. The large barriers in injecting electrodes of devices would result to higher driving and operating voltage and lower efficiency [5]. The decreasing of hole injection barrier from ITO electrode can solve this problem and over the past two decades, most efforts have been done for this purpose [6]. Among these efforts, the use of transition metal oxides (TMOs) has been considered to improve the OLED performance. For example, tungsten oxide (WO_3) [7], vanadium pent-oxide (V_2O_5) [8], iron oxide (Fe_3O_4) [9, 10], nickel oxide (NiO) [11, 12], copper oxide (CuO) [13] and rhenium trioxide (ReO_3) [14], were used as an inorganic hole-injection layer (HIL) between anode (ITO) and organic HTL. Due to semiconducting properties of these materials and other interesting properties, such as high work functions and good

transparency, they are very important for using as HIL which can lead to the reduction of holes injection barrier. For example, The ITO work function (WF) is considered as 4.7 eV (or 5.1 eV when it is influenced by oxygen plasma or UV-zone) and the highest occupied molecular orbital (HOMO) of organic hole-transport material such as N-N-diphenyl-N,N-(bis(3-methylphenyl)-1,10-biphenyl-4,40-diamine) (TPD) is considered as 5.4 eV [15–17], thus there is a large injection barrier for hole injection in ITO / TPD interface.

The WF of MoO_3 (6.9eV) is much lower than HOMO level of TPD [18] and has interesting optical, electrical and thermal properties such as transparency in visible range, moderate conductivity (semiconductor) and relatively low evaporation temperature. Also the existence of gap states in MoO_3 and locating the HOMO level of TPD in the band gap of MoO_3 leads to the reduced injection barrier for holes from ITO to TPD layer. Thus, this semiconductor can be used as HIL between anode (ITO) and HTL (TPD) [19- 21].

In this work, to investigate about influence of the MoO_3 thicknesses on the hole injection from ITO anode to TPD (HTL) and consequently on the performance of OLED devices, MoO_3 HILs with thicknesses of 1 nm, 5 nm and 20 nm with thermal evaporation technique have been deposited. The results of current density- luminance-voltage characteristics of these devices show that with using a 5nm-thick MoO_3 as HIL, the electrons would transfer from ITO and TPD to MoO_3 and in conclusion the formation of an ohmic contact at ITO/ MoO_3 /TPD interfaces would be possible. This would provide the lowest driving and operating voltage compared to OLED

devices with other MoO₃ thicknesses. Thus the best thickness for MoO₃ HIL in the proposed OLED devices is 5 nm.

2. Experimental

The ITO-coated glass as anode, TPD as HTL and Alq₃ as EML and ETL are provided from sigma Aldrich Company and MoO₃ as HIL, LiF as EIL and Al as cathode are provided from other companies. Then, OLEDs are fabricated at various thicknesses of the MoO₃, based on the following steps: All OLED devices are prepared on ITO-coated glass substrates with a resistance of 20 Ω/square with the structure of ITO/MoO₃ (x nm, where x=0, 1, 5, 20)/TPD (40 nm)/Alq₃(38 nm)/LiF(0.5 nm)/Al(100 nm). Before fabrication of devices, the ITO substrates are patterned into two stripes using hydrochloric acid, and zinc powder for etching. They are then ultrasonically cleaned using detergent, acetone, ethanol and de-ionized water, each with a 15 min interval. In the subsequent step of the ITO cleaning process, the N₂ gas is used to obtain dried substrates. The cleaned substrates are set in a thermal evaporation system at base pressure of 3×10⁻⁶ mbar. At this pressure, all layers are successively vacuumed and deposited on the ITO anode layer. For controlling the Deposition rates, a quartz crystal located above the thermal boats, is used which controls the values of 0.1 Å/s for MoO₃, 0.1-0.7 Å/s for TPD and Alq₃, 0.1 Å/s for LiF and 1-5 Å/s for Al. The active area of the OLED devices was about 50 mm². For measuring the Current density–voltage–luminance (J–V–L) characteristics of the OLED devices in ordinary conditions, an I-V meter connected to a computer and commercial light meter prepared with a calibrated silicon photodiode is used.

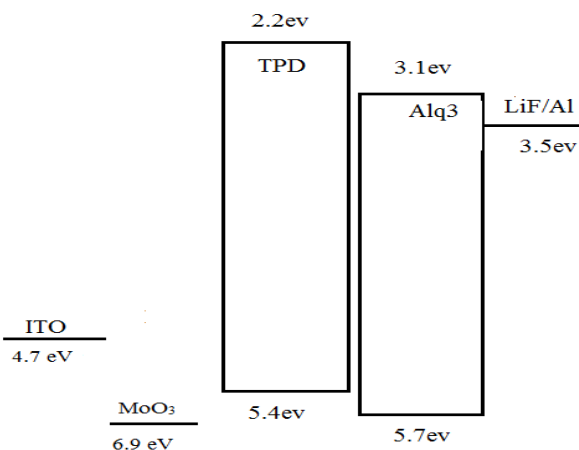


Fig. 1. the schematic view of Energy band diagram of OLED

3. Results and discussions

Current Density–Voltage (J–V) and Luminance–Voltage (L–V) characteristics of EL devices are shown in Figs. 2 and 3, respectively. These figures show that the presence of MoO₃ buffer layer (1 nm, 5 nm and 20 nm) leads to shift of J–V and L–V curves toward lower voltages compared with the reference device (without MoO₃ buffer layer). In Fig. 2, the shift of J–V curves for an OLED device with MoO₃=5 nm is the highest, while for other device with MoO₃=20 nm is the lowest. In Fig. 3, the shift of L–V curves for an OLED device with MoO₃=5 nm is the highest, while for other device with MoO₃=1 nm is the lowest. In Fig. 4, the turn-on voltage (operating voltage at 1cd/m²) of the reference device is 4V while for other devices (MoO₃= 1 nm, 5 nm and 20 nm) is decreased to a lower value of 3.5V which is due to the energy barrier reduction at the anode/HTL interface. Also, this figure shows that the operating voltages of MoO₃ devices at three values of luminance (78,120 and 135cd/m²) are lower than the reference device. The device with MoO₃=5 nm shows the lowest operating voltage, whereas the device with MoO₃=1 nm represents the highest operating voltage among MoO₃ devices. In Fig. 5, the driving voltages of MoO₃ devices (1 nm, 5 nm and 20 nm) at three values of current density (27A/m², 37 A/m² and 50A/m²) are lower than the reference device. The device with MoO₃=5nm has the lowest driving voltage, while the device with MoO₃=20 nm has the highest driving voltage among all MoO₃ devices. These results indicate that the optimized value for MoO₃ buffer layer thickness would be 5 nm and the superior holes injection and transportation, resulting from insertion of MoO₃ HIL, has been led to EL enhancement of devices.

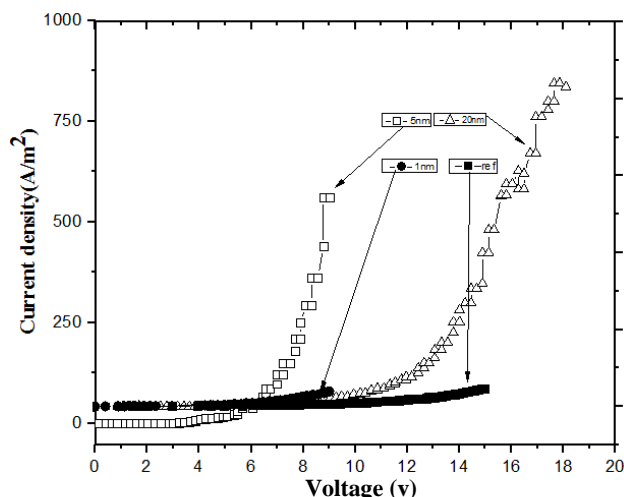


Fig. 2. Current density-Voltage characteristic of the OLED devices with MoO₃ thicknesses varying from 0 to 20 nm

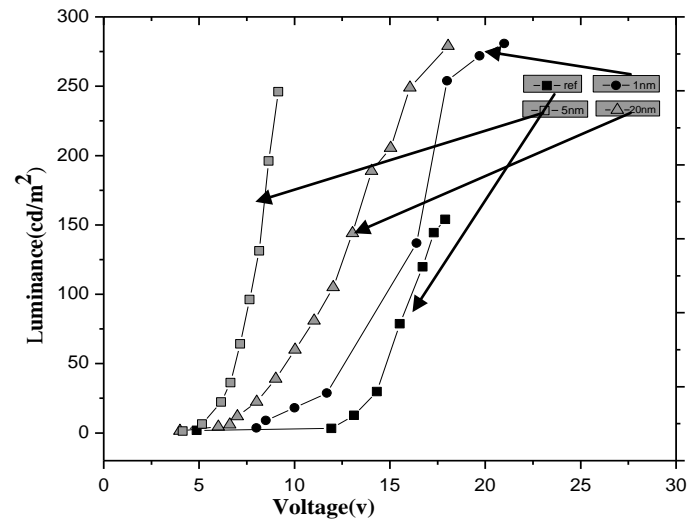


Fig. 3. Luminance - Voltage characteristic of the OLED devices with MoO_3 thicknesses varying from 0 to 20 nm

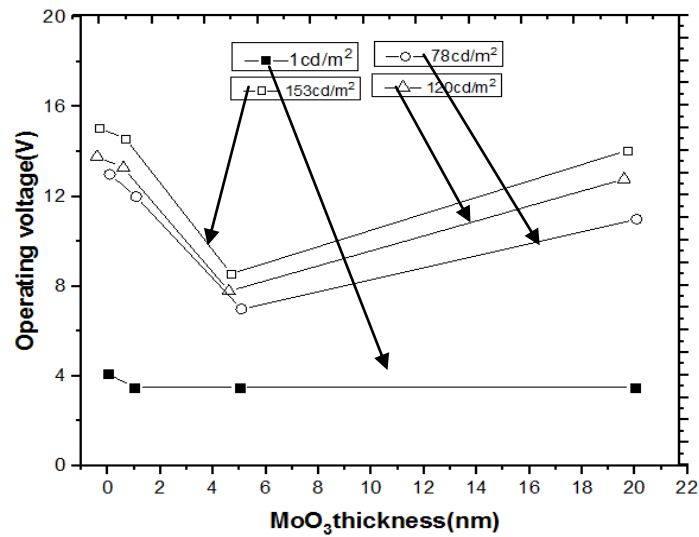


Fig. 4. The turn-on voltage (operating voltage at Luminance of 1 cd/m^2) and operating voltages of OLED devices in terms of MoO_3 thickness at three values for luminance ($L=78, 120, 153 \text{ cd/m}^2$)

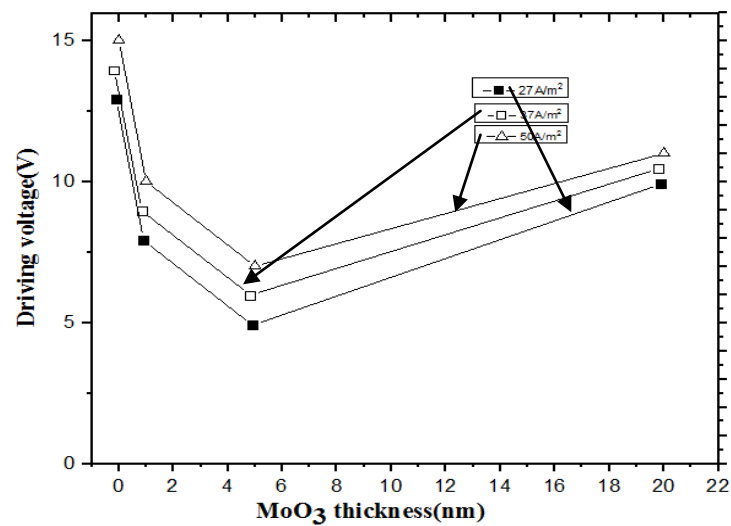


Fig. 5. The driving voltage of OLED devices in terms of MoO_3 thickness at three value for current density ($J=27,37,50 \text{ A/m}^2$)

The Figs. 6 and 7 show that the insertion of MoO₃ (1 nm, 5 nm and 20 nm) buffer layer leads to decreasing of current efficiency and power efficiency of OLED devices with respect to reference device at two values of current density (30 A/m² and 40 A/m²). The devices with MoO₃=5 nm and MoO₃=20 nm have the lowest and highest current and power efficiencies among MoO₃ devices respectively.

This is related to driving voltage of MoO₃ devices. In devices with MoO₃=5 nm, due to the lowest driving voltage and increasing of the hole injection, the balances of charge carrier would destroy but in device with MoO₃=20 nm, due to highest driving voltage, this situation would improve.

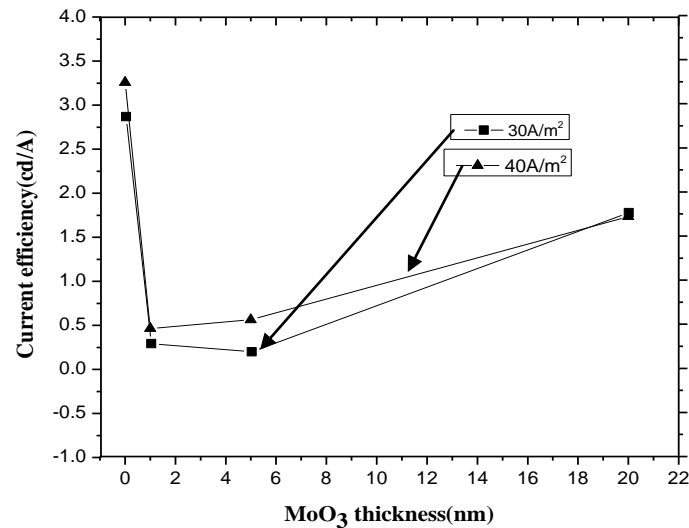


Fig. 6. The current efficiency of OLED devices in terms of MoO₃ thickness at two value of current density

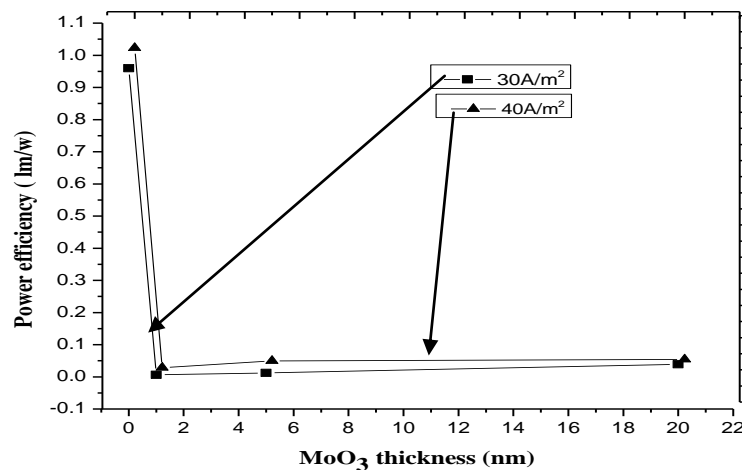


Fig. 7. The power efficiency of OLED devices in terms of MoO₃ thickness at two value of current density

Fig. 8 shows that in MoO₃ (1 nm and 5 nm) devices, the values of area roughness for ITO/MoO₃ (1 nm) and ITO/MoO₃ (5 nm) films ($R_a=2.23$ nm and $R_a=2.64$ nm respectively) do not increase highly with respect to area roughness of ITO film ($R_a=2.12$ nm) in reference device. This shows the formation of uniform layer of MoO₃ on the ITO substrate as the formation of uniform layer of ITO on the glass substrate. Thus the enhancement of performance for MoO₃ (1 nm and 5 nm) devices, could be related to decreasing of the hole injection barrier with maintaining the smooth morphology of the deposited

MoO₃ films which improve the interfacial contact between the ITO anode and HTL. But the performance of MoO₃ (20 nm) device is destroyed in compared with other MoO₃ devices, due to high value of area roughness ($R_a=5.84$ nm) and formation of non uniform MoO₃ films (the existence of grains). However, the performance of this device is better than the reference device despite higher value for area roughness of ITO/MoO₃ (20 nm) film ($R_a=5.84$ nm) in this device with respect to area roughness of ITO films ($R_a=2.12$ nm) in reference device due to reduced hole injection barrier in MoO₃ devices.

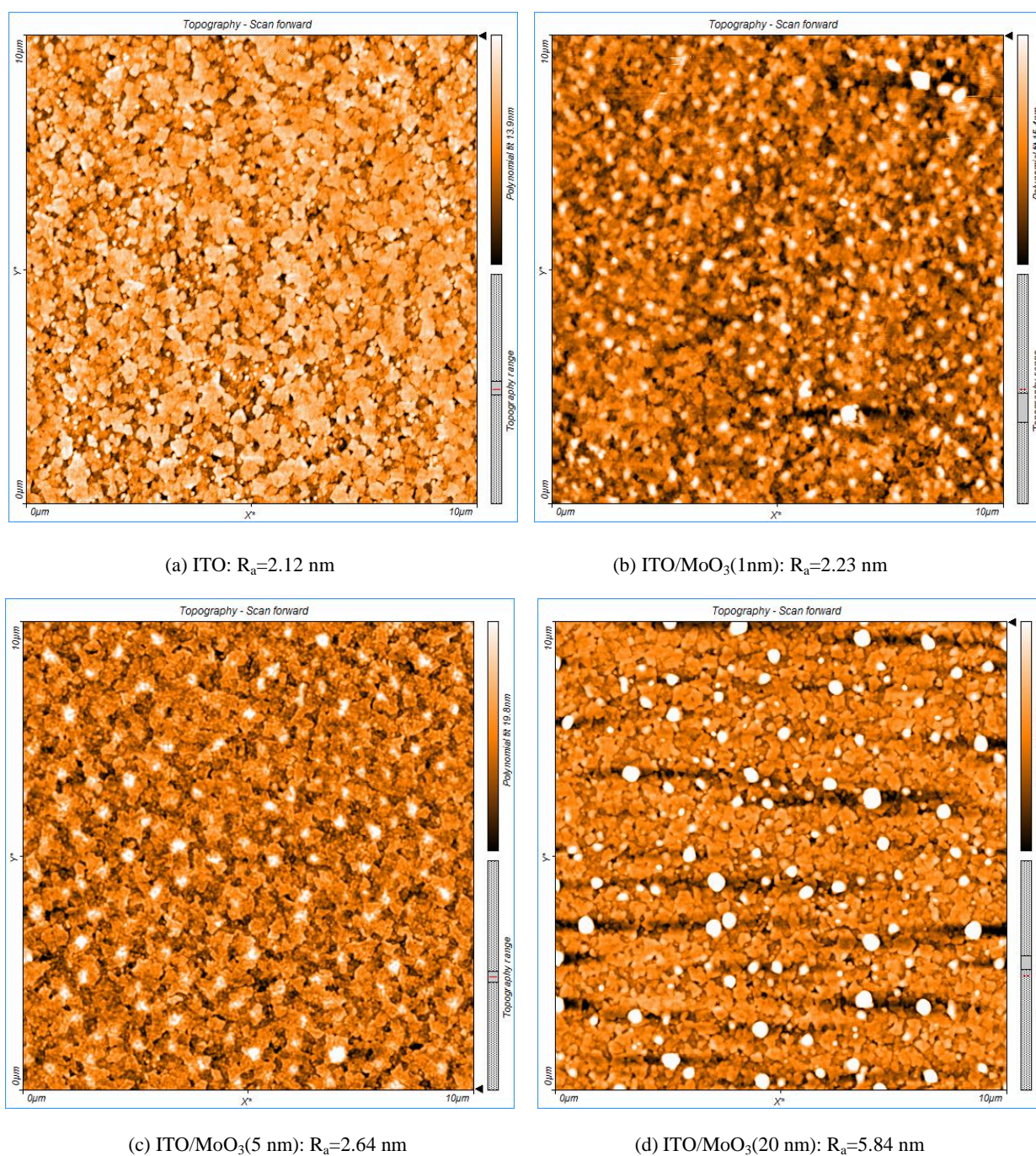


Fig. 8. AFM images of ITO and ITO/ MoO_3 films with different thicknesses of MoO_3

In continuation of this study, the reasons of these experimental observations have been investigated with considering the HOMO level of TPD (5.4 eV), work function of ITO (4.7 eV), effective work function of MoO_3 (5.2 eV) and the existence of gap states in MoO_3 as follows:

The gap states of MoO_3 contribute in hole injection and transportation from ITO anode to TPD (HTL) and formation of dipole layers at the ITO/ MoO_3 and MoO_3 /TPD interfaces. These dipoles lead to decreasing of the work function of MoO_3 from 6.9 eV to effective value

of 5.2 eV. This value which is located between work function of ITO (4.7 eV) and HOMO level of TPD (5.4 eV) leads to decreasing of the hole injection barrier from ITO anode to TPD (HTL) and in conclusion decreasing of the driving and operating voltages. However for devices with thicker MoO_3 buffer layer ($\text{MoO}_3=20$ nm), the formation of strong interfacial dipole layers with respect to devices with $\text{MoO}_3=5$ nm leads to increasing of the driving and operating voltage [22-24]. For devices with thinner MoO_3 buffer layer ($\text{MoO}_3=1$ nm), the gap states do not contribute in hole injection and transportation and in

this case, the hole injection has been occurred through the tunneling mechanism [25, 26].

4. Conclusions

The insertion of MoO₃ (1 nm, 5 nm and 20 nm) as HIL leads to shift of J-V and L-V curves toward lower voltages (decreasing of the turn-on, operating and driving voltages) in comparison with reference device (without MoO₃ buffer layer). The device with MoO₃=5 nm, has the lowest driving and operating voltage, the device with MoO₃=20 nm has the highest driving voltage and the device with MoO₃=1nm has the highest operating voltage among MoO₃ devices. Thus the device with MoO₃=5 nm has the best performance among all OLED devices from the point of operating and driving voltage view. Also, the insertion of MoO₃ as HIL has been led to decreasing of current efficiency and power efficiency for MoO₃ devices in comparison with reference device. The devices with MoO₃=5 nm and MoO₃=20 nm have the lowest and highest current and power efficiencies among MoO₃ devices respectively. These results are related to the HOMO level of TPD, work functions of MoO₃ and ITO, gap states in MoO₃, interfacial dipoles and morphology of the MoO₃ films.

References

- [1] C. W. Tang, S. A. VanSlyke, C. H. Chen, *J. Appl. Phys.* **65**(9), 3610 (1989).
- [2] C. W. Tang, S. A. VanSlyke, *Appl. Phys. Lett.* **51**(12), 913 (1987).
- [3] M.-C. Sun, J.-H. Jou, W.-K. Weng, Y.-S. Huang, *Thin Solid Films* **491**(1–2), 260 (2005).
- [4] A. Bahari, M. Roodbari Shahmiri, M. Derakhshi, M. Jamali, *J. Nanostructures* **2**(3), 313 (2012).
- [5] S.-F. Chen, C.-W. Wang, *Appl. Phys. Lett.* **85**(5), 765 (2004).
- [6] H. You, Y. Dai, Z. Zhang, D. Ma, *J. Appl. Phys.* **101**(2), 26105 (2007).
- [7] M. J. Son, S. Kim, S. Kwon, J. W. Kim, *Org. Electron.* **10**(4), 637 (2009).
- [8] J. Meyer, K. Zilberberg, T. Riedl, A. Kahn, *J. Appl. Phys.* **110**(3), 33710 (2011).
- [9] D. D. Zhang, J. Feng, H. Wang, Y. Bai, Q. D. Chen, S. Y. Liu, H. B. Sun, *Appl. Phys. Lett.* **95**, 263303 (2009).
- [10] D. D. Zhang, J. Feng, Y. Q. Zhong, Y. F. Liu, H. Wang, Y. Jin, Y. Bai, Q. D. Chen, H. B. Sun, *Org. Electron.* **11**, 1891 (2010).
- [11] I. M. Chan, T. Y. Hsu, F. C. Hong, *Appl. Phys. Lett.* **81**, 1899 (2002).
- [12] B. Wei, S. Yamamoto, M. Ichikawa, C. Li, T. Fukuda Y. Taniguchi, *Semicond. Sci. Technol.* **22**, 788 (2007).
- [13] G. B. Murdoch, M. Greiner, M. G. Helander, Z. B. Wang, Z. H. Lu, *Appl. Phys. Lett.* **93**, 083309 (2008).
- [14] D.-S. Leem, H.-D. Park, J.-W. Kang, J.-H. Lee, J. W. Kim, J.-J. Kim, *Appl. Phys. Lett.* **91**(1), 011113 (2007).
- [15] D.-D. Zhang, J. Feng, Y.-F. Liu, Y.-Q. Zhong, Y. Bai, Y. Jin, G.-H. Xie, Q. Xue, Y. Zhao, S.-Y. Liu, H.-B. Sun, *Appl. Phys. Lett.* **94**(22), 223306 (2009).
- [16] D. Kalhor, E. Mohajerani, O. Hashemi Pour, *Journal of Luminescence* **167**, 376 (2015).
- [17] H. Zhang, Y. Dai, D. Ma, H. Zhang, *Appl. Phys. Lett.* **91**(12), 123504 (2007).
- [18] M. Kröger, S. Hamwi, J. Meyer, T. Riedl, W. Kowalsky, A. Kahn, *Appl. Phys. Lett.* **95**(12), 123301 (2009).
- [19] S. R. Hammond, J. Meyer, N. E. Widjonarko, P. F. Ndione, A. K. Sigdel, A. Garcia, A. Miedaner, M. T. Lloyd, A. Kahn, D. S. Ginley, J. J. Berry, D. C. Olson, *J. Mater. Chem.* **22**(7), 3249 (2012).
- [20] J. Meyer, S. Hamwi, T. Bülow, H.-H. Johannes, T. Riedl, W. Kowalsky, *Appl. Phys. Lett.* **91**(11), 113506 (2007).
- [21] S. Tokito, K. Noda, Y. Taga, *J. Phys. D: Appl. Phys.* **29**(11), 2750 (1996).
- [22] H. Lee, S. W. Cho, K. Han, P. E. Jeon, C.-N. Whang, K. Jeong, K. Cho, Y. Yi, *Appl. Phys. Lett.* **93**(4), 43308 (2008).
- [23] K. Kanai, K. Koizumi, S. Ouchi, Y. Tsukamoto, K. Sakanoue, Y. Ouchi, K. Seki, *Org. Electron.* **11**(2), 188 (2010).
- [24] T. Matsushima, H. Murata, *Appl. Phys. Lett.* **95**(20), 203306 (2009).
- [25] X. Haitao, Z. Xiang, *J. Appl. Phys.* **114**, 244505 (2013).
- [26] T. Matsushima, G. H. Jin, H. Murata, *J. Appl. Phys.* **104**, 054501 (2008).

*Corresponding author: auobi_ali@yahoo.com